# Hepatic gene expression and functional changes associated with nonalcoholic steatohepatitis

KANA MATSUMOTO[1], YUMIKO KATO[2], MOMONE HAYASHI[2], RISA MIURA[1], SATORU MONZEN[3] and MITSURU CHIBA[1]

[1]Department of Bioscience and Laboratory Medicine, Graduate School of Health Sciences; [2]Department of Medical Technology, School of Health Sciences; [3]Department of Radiation Sciences, Graduate School of Health Sciences, Hirosaki University, Hirosaki, Aomori 036-8564, Japan

Received April 1, 2022; Accepted July 21, 2022

DOI: 10.3892/mmr.2022.12841

**Abstract.** Non-alcoholic steatohepatitis (NASH) is a pathological condition of the liver in which hepatocyte steatosis, invasion of inflammatory cells and hepatic injury occur without alcohol abuse. Despite the known risk of liver cancer and liver fibrosis that may progress to liver cirrhosis that exists with NASH, an understanding of related gene expression and associated functional changes remains insufficient. The present study used a mouse model of NASH induced by a high-fat diet to examine gene expression in the liver and to search for transcripts that could predict early liver fibrosis in the future. Mice fed a high-fat diet for 2 weeks showed typical NASH liver histology by hematoxylin and eosin staining, and increased fibrosis was confirmed by Sirius red staining after 6 weeks. Functional changes associated with liver damage, liver inflammation, liver steatosis and liver fibrosis were predicted by toxicological ontology analysis using Ingenuity Pathways Analysis. Downregulated microRNA (miR)-21 and upregulated *collagen type III α1* mRNA in the liver and upregulated exosomal miR-21 in serum of mice fed a high-fat diet for 1 and/or 2 weeks were confirmed by reverse transcription-quantitative PCR, suggesting that these changes occur prior to histological confirmation of fibrosis. Therefore, it may be possible to predict future liver fibrosis by analyzing fibrosis-related genes that shift prior to pathological findings.

## Introduction

Nonalcoholic fatty liver disease (NAFLD) is a disorder involving excess fat buildup in the liver. Causes of NAFLD include insulin resistance, lifestyle diseases, abnormal lipid metabolism, endocrine diseases, etc. Individuals with this condition have fatty deposits in the liver without excessive alcohol use (1). NAFLD is a risk factor for the development of lifestyle-related diseases and should be regarded as a systemic disease since obesity and lifestyle-related diseases are frequently associated (1,2). Classifications of NAFLD include nonalcoholic fatty liver, which develops based on large-drop fat degeneration and rarely progresses, and nonalcoholic steatohepatitis (NASH), which is progressive and can result in liver cirrhosis and hepatocellular carcinoma (3).

NASH is a pathological condition of NAFLD in which fatty degeneration, inflammatory cell infiltration, and hepatocellular injury (balloon-like degeneration) are observed (4-6). Currently, it is estimated that ~25% of the world population has NAFLD, with a high prevalence in obese and diabetic subjects (7,8). The risk of progression to cirrhosis and liver cancer is a problem in cases with highly advanced fibrosis (9,10). Unfortunately, a promising marker of initial fibrosis and a test method that can predict future fibrosis has yet to be discovered.

In our previous study, we showed that various mRNA and non-coding RNA expression changes occur in human liver cancer patient tissues and can be classified by disease stage (11). Previously, it was also suggested that microRNAs are altered in the NASH liver, and miR-122 and miR-192 appear in the blood, which may serve as biomarkers for NASH (12). Therefore, gene expression in NASH liver tissue and blood samples could be examined to predict future fibrosis. In this study, we used a mouse model of NASH induced by a high-fat diet to examine gene expression in the liver and to search for transcripts that could predict early liver fibrosis in the future.

## Materials and methods

*Animals*. Five-week-old C57BL/6NJcl male mice were purchased from Clea Japan and acclimatized for 1 week before starting the experiment. Food and water were fed ad libitum to the mice and changed every two to three days. The bedding was changed once a week. The mice were fed a choline-deficient, L-amino acid-defined, high-fat diet (CDAHFD, A06071302, RESEARCH DIETS) consisting of 60 kcal% fat and 0.1%

*Correspondence to:* Dr Mitsuru Chiba, Department of Bioscience and Laboratory Medicine, Graduate School of Health Sciences, Hirosaki University, 66-1 Hon-cho, Hirosaki, Aomori 036-8564, Japan
E-mail: mchiba32@hirosaki-u.ac.jp

*Key words:* non-alcoholic steatohepatitis, gene expression, microarray, miR-21, collagen type III α1

methionine by weight to induce the onset of NASH (13). A dietary breeding solid-type feed CE-2 (Clea Japan) was fed to a control mouse group under the same conditions other than the diet. A sampling of six animals in each control and NASH group was performed at 1, 2, and 6 weeks. One mouse from each group had the liver removed after perfusion fixation with 4% paraformaldehyde, and the other four or five had the liver removed after cardiac blood sampling. All experiments were performed under anesthesia with the inhalation anesthetic solution isoflurane (Pfizer Inc.). Anesthesia was introduced by inhalation with a small animal anesthesia machine (Muromachi Kikai) vaporized to a concentration of 4-5% and maintained at 2-3%. Cervical dislocation was used for euthanasia after liver removal, and death was confirmed by cessation of respiration and heartbeat. Liver samples were stored at -80˚C immediately after collection, and blood samples were serum separated immediately after collection. All animal experiments were performed in accordance with the Guidelines for Animal Experimentation of Hirosaki University, and complied with the ARRIVE guidelines and the AVMA euthanasia guidelines 2020. The procedures were approved by The Animal Research Committee of Hirosaki University (approval nos. G18002).

*Hematoxylin and eosin staining*. Paraffin-embedded tissue was thin sliced at 4 $\mu$m. The slide glass to which the paraffin-embedded section was attached was deparaffinized, treated for hydrophilicity, and washed with water. After 1 min, Mayer's hematoxylin solution (Wako) was applied to dye the nuclei, and the excess color was rinsed with warm water for 10 min. After staining with 0.5% eosin Y/ethanol solution (Wako) for 10 sec, the slides were washed with water to remove excess staining solution and separated with 75% ethanol. Specimens were dehydrated with ethanol, rendered transparent with xylene, and mounted with Marinol (Muto Chemical Co., Ltd.) and cover glass (Matsunami Glass Industry Co.). The stained slides were visualized under visible light using a BZ-X700 microscope (KEYENCE).

*Sirius red staining*. Slides with paraffin-embedded sections attached were deparaffinized, treated for hydrophilicity, and washed with running water for 5 min. After dyeing with Sirius red solution for 10 min, the color was rinsed with water for 5 min, then dehydrated with ethanol, rendered transparent with xylene, and mounted with Marinol (Muto Kagaku Co., Ltd.) and cover glass (Matsunami Glass Industry Co.). The stained slides were visualized under visible light using a BZ-X700 microscope (KEYENCE).

*Immunohistochemistry staining*. Slides with paraffin sections attached were deparaffinized, treated for hydrophilicity, and washed with water for 5 min. Slides were treated with 3% $H_2O_2$ for 5 min to inactivate the endogenous peroxidase and washed with water for 5 min. For antigen activation, the slides were placed in a heat-resistant doze filled with citric acid buffer (pH 6.0) and autoclaved at 115˚C for 5 min. The slides were washed with TBS buffer (25 mM Tris-HCl and 150 mM NaCl, pH 7.2) for 5 min and treated with blocking solution (5% goat serum in TBS buffer) at room temperature for 30 min. Next, the slides were incubated with the blocking solution containing a primary rabbit monoclonal antibody directed against α-smooth muscle actin (α-SMA) (Cell Signaling Technology) at a 1:500 dilution at room temperature for 60 min, then washed three times with TBS buffer, and incubated at room temperature for 60 min with EnVision +System-HRP Labelled Polymer Anti-Rabbit (Dako). The slides were washed three more times with TBS buffer and stained with 3,3'-diaminobenzidine and Mayer's hematoxylin solutions.

*RNA extraction*. RNAs from livers, serum and serum exosomes were extracted using the Isogen II reagent (Nippon gene), according to the manufacturer's instructions. The quality and concentration of total RNAs from livers were assessed using a NanoDrop spectrophotometer (NanoDrop Technologies). All RNA samples had 260/280 nm absorbance ratios of 1.8-2.0. The concentration of RNAs from serum and serum exosomes was measured using Qubit™ 4 Fluorometer and Qubit™ microRNA Assay kit (Thermo Fisher Scientific, Inc.).

The peaks of total RNAs were confirmed using an Agilent 2100 Bioanalyzer and an Agilent RNA 6000 Pico Kit (Agilent Technologies), according to the manufacturer's instructions.

*Microarray analysis*. Cyanine 3 (Cy3)-labeled complementary RNA (cRNA) was synthesized from 150 ng of liver total RNA using a Low Input Quick Amp Labeling Kit (Agilent Technologies), according to the manufacturer's instructions. The synthesized Cy3-labeled cRNA was hybridized with a microarray slide (SurePrint G3 Mouse GE 8x60 K Microarray Kit; Agilent Technologies) at 65˚C for 17 h. After hybridization, the slides were washed with the Gene Expression Wash Pack (Agilent Technologies). Cy3 fluorescence signals were detected with a SureScan Microarray Scanner (Agilent Technologies). Fluorescent images were quantified using Feature Extraction software (Agilent Technologies). GeneSpring 14.5 software (Agilent Technologies) was used for normalization and expression analysis. Genes showing an expression level fold change >1.5 or higher were analyzed by comparing the control and NASH groups. Function prediction was performed using Ingenuity Pathway Analysis (IPA) (Qiagen).

*Real-time PCR*. The expression of mouse collagen type III α1 (Col3a1) and glyceraldehyde-3-phosphate dehydrogenase (Gapdh) mRNAs in mouse liver was determined by real-time PCR. Complementary DNA (cDNA) was synthesized from total RNA using the Applied Biosystems™ High-Capacity cDNA Reverse Transcription Kit (Thermo Fisher Scientific, Inc.), according to the manufacturer's instructions. Quantitative polymerase chain reaction (qPCR) was performed using a Power SYBR Green PCR Master Mix (Thermo Fisher Scientific, Inc.), 10 $\mu$M of forward and reverse primer pairs, and the StepOne Plus Real-time PCR System (Thermo Fisher Scientific, Inc.) under the following conditions: 10 min at 95˚C, followed by 45 cycles each of 95˚C for 15 sec, and 60˚C for 60 sec with *Gapdh* used as an internal control.

The expression level of miR-21 in mouse liver, serum and serum exosomes was examined by real-time PCR. Exosomes from serum were extracted using Total Exosome Isolation from serum (Thermo Fisher Scientific, Inc.). The cDNAs from miR-21 were synthesized using the TaqMan™ miRNA RT Kit and the prescribed 5x RT primer (both from Thermo Fisher Scientific, Inc.), according to the manufacturer's instructions. The qPCR for miR-21 was performed using a FastStart

TaqMan probe master (Roche Diagnostics), a 20x probe, and the StepOne Plus Real-Time PCR System (Thermo Fisher Scientific, Inc.) under the following conditions: 10 min at 95˚C, followed by 45 cycles at 95˚C for 15 sec, and 60˚C for 60 sec with U6 snRNA as an internal control and cel-miR-39 as an external control. The comparative Ct method was used to determine expression levels.

*Statistical analysis*. Statcel 3 software (OMS Publishing Inc., Saitama, Japan) was used to perform all statistical analyses. Unpaired Student's t-test was performed to compare the results of the two groups. $P<0.05$ was considered a statistically significant difference.

## Results

*Histological changes in mouse NASH livers*. We harvested the livers of control and NASH mice at 1, 2, and 6 weeks after high-fat diet intake for histological analysis to confirm the model. The livers of the control group mice were histologically normal at all time points. In contrast, the livers of the NASH mice showed hepatocellular damage and fat droplets and the appearance of inflammatory cells by hematoxylin and eosin staining after 2 and 6 weeks. At 1 week, some of the NASH group showed changes (Fig. 1A). Sirius red staining and α-SMA immunostaining revealed increasing fibers and activated star cells in NASH mice 6 weeks after ingesting the high-fat diet (Fig. 1B and C). These results indicate that the entire liver is in a NASH state after 2 weeks of high-fat diet intake and that liver fibrosis occurs at 6 weeks.

*Gene expression changes in mouse NASH livers*. To investigate the changes in gene expression associated with NASH development, we performed mRNA microarray analysis. We investigated genes with >1.5-fold difference in expression in the NASH group compared to the control group. Mice at 1 week without complete NASH, 2 weeks with NASH, and 6 weeks with advanced fibrosis were selected for analysis.

The numbers of genes upregulated more than 1.5-fold in the livers of NASH mice compared to control mice were 2912, 2684 and 2791 in 1, 2 and 6 weeks, respectively (Fig. S1). Whereas, the numbers of genes downregulated more than 1.5-fold in the livers of NASH mice compared to control mice were 5243, 4288 and 4591 in 1, 2 and 6 weeks, respectively (Fig. S1). These suggest that numerous gene expressions are altered by the onset of NASH. The microarray data used in this study were registered with Gene Expression Omnibus (GSE200409).

*Functional change prediction by IPA*. Based on the mRNA expression data of mouse livers at 1, 2, and 6 weeks, we used IPA toxicity ontology analysis to predict functional changes and determine which expressed genes affect biological functions and diseases. Increased liver damage, liver inflammation, liver steatosis and liver fibrosis was shown as a predicted function. In addition, when we compared the histological findings with the time when the cells started to show hyperfunction by gene expression, there was a general agreement between the two (Table I). Interestingly, fibrosis was not clearly visible in the histological findings until 6 weeks, but functional prediction by gene expression was forecast to increase at 2 weeks.

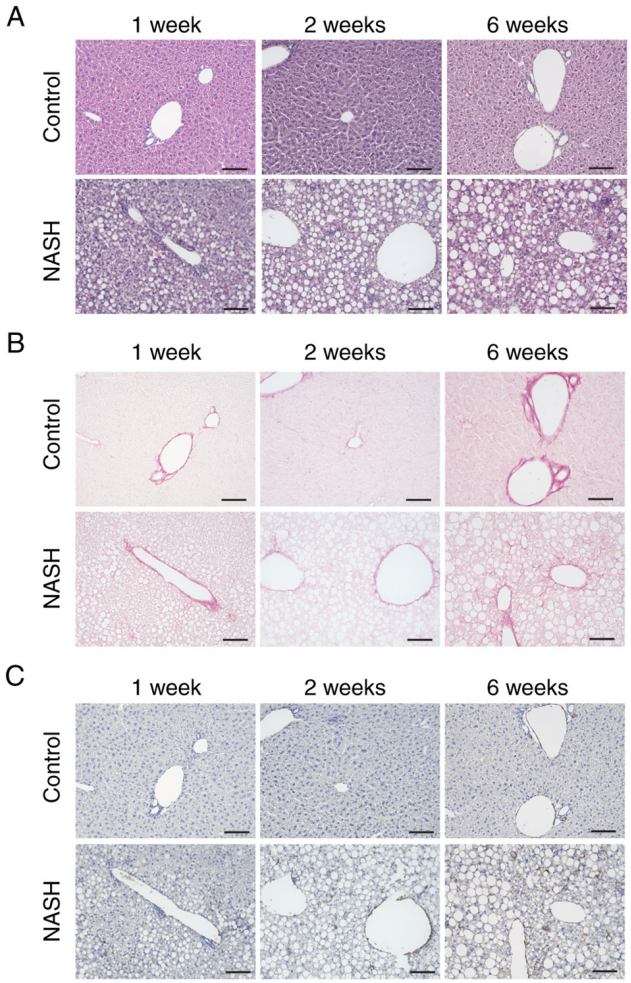


Figure 1. Histological liver images of control and NASH groups at 1, 2 and 6 weeks. (A) Hematoxylin and eosin staining: In the NASH group, numerous small vacuoles in the liver parenchyma and fatty degeneration were observed. The NASH group also showed hepatocyte ballooning and inflammatory cell infiltration. The three characteristics of NASH were confirmed after 2 weeks. (B) Sirius red staining: In the NASH group, fibrosis was observed in the liver parenchyma at 6 weeks. (C) α-SMA immunostaining: In the NASH group, partial activation of astrocytes was observed at 2 weeks and overall activation at 6 weeks. Scale bars, 100 $\mu$m. NASH, non-alcoholic steatohepatitis.

As for liver fibrosis, the increase in the number of molecules associated with fibrosis between 1 and 2 weeks was more pronounced than at 6 weeks when histological findings confirmed fibrosis. In addition, the Venn diagram of common liver fibrosis-related expressed genes showed that there were 11 genes common in all weeks (Fig. 2). Changes in common genes and expression levels at 1, 2, and 6 weeks are shown in Table II. There were 54 genes in common between 2 and 6 weeks, and there was little difference in the number of genes between 2 and 6 weeks. This finding suggests that changes in gene expression associated with the pathogenesis of NASH occur as early as 1 week and the expression of fibrosis-associated molecules is already increased from 1 or 2 weeks when a clear fibrosis image is observed on pathological examination at 6 weeks.

*Prediction of upstream regulatory molecules by IPA upstream analysis*. To investigate the upstream molecules involved in the changes in gene expression, we performed

Table I. Comparison of histological findings and functional prediction by Ingenuity Pathway Analysis.

| Time after high-fat diet intake | Liver damage | | Liver inflammation | | Liver steatosis | | Liver fibrosis | |
|---|---|---|---|---|---|---|---|---|
| | Histological findings | Functional prediction | Histological findings | Functional prediction | Histological findings | Functional prediction | Histological findings | Functional prediction |
| 1 week | Damage | Hyperfunction | Partial fatidation | No sign | Non-fibrosis | Mild hyperfunction | Non-fibrosis | Mild hyperfunction |
| 2 weeks | Damage | Hyperfunction | Fatidation | Hyperfunction | Mild fibrosis | Hyperfunction | Mild fibrosis | Hyperfunction |
| 6 weeks | Significant damage | Hyperfunction | Fatidation | Hyperfunction | Fibrosis | Hyperfunction | Fibrosis | Hyperfunction |

Table II. Changes in gene expression of fibrosis-related genes at 1, 2 and 6 weeks.

| | Fold-change | | |
|---|---|---|---|
| Genes | 1 week | 2 weeks | 6 weeks |
| *Adk* | 48.87 | -1.75 | -1.94 |
| *Adora2a* | 1.59 | 1.59 | 3.27 |
| *Col3a1* | 4.74 | 6.74 | 9.61 |
| *Golm1* | 2.62 | 4.97 | 4.88 |
| *Gstp1* | -3.28 | -2.50 | -2.57 |
| *Ifnar2* | -1.66 | -1.63 | -1.63 |
| *Impdh1* | 1.86 | 2.16 | 2.02 |
| *Pdgfrb* | 1.80 | 2.00 | 3.33 |
| *Srebf1* | -2.56 | -2.66 | -2.05 |
| *Tgfb1* | 1.93 | 2.35 | 2.67 |
| *Tlr4* | 1.80 | 2.73 | 2.64 |

Adk, adenosine kinase; Adora2a, adenosine A2a receptor; Col3a1, collagen type III α1; Golm1, golgi membrane protein 1; Gstp1, glutathione S-transferase, pi1; Ifnar2, interferon (α and β) receptor 2; Impdh1, inosine monophosphate dehydrogenase 1; Pdgfrb, platelet derived growth factor receptor, β polypeptide; Srebf1, sterol regulatory element binding transcription factor 1; Tgfb1, transforming growth factor, β1; Tlr4, toll-like receptor 4.

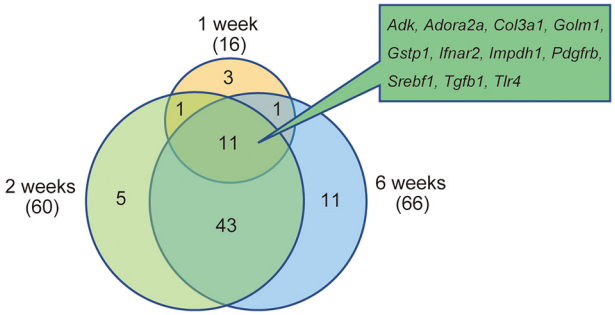


Figure 2. Toxic ontology analysis of diseases and functions by Ingenuity Pathway Analysis. Venn diagram of liver fibrosis-related genes. The genes associated with liver fibrosis in Table II are presented in the Venn diagram. NASH, non-alcoholic steatohepatitis; *Adk*, adenosine kinase; *Adora2a*, adenosine A2a receptor; *Col3a1*, collagen type III α1; *Golm1*, golgi membrane protein 1; *Gstp1*, glutathione S-transferase, pi1; *Ifnar2*, interferon (α and β) receptor 2; *Impdh1*, inosine monophosphate dehydrogenase 1; *Pdgfrb*, platelet derived growth factor receptor, β polypeptide; *Srebf1*, sterol regulatory element binding transcription factor 1; *Tgfb1*, transforming growth factor, β1; *Tlr4*, toll-like receptor 4.

IPA upstream analysis. The upstream molecules predicted to be involved in the activation or repression of gene expression are shown in Fig. S2. Among the upstream molecules, transcription regulators, kinase, and enzyme changes were particularly common. Among the upstream regulatory molecules, we focused on miRNAs as promising biomarkers that can be measured in the blood (Table III and Fig. S2). The findings suggest that various upstream regulatory molecules, including microRNAs, are involved in the expression changes of NASH-related genes.

Table III. Prediction of upstream regulatory miRNAs by upstream analysis.

| Prediction | 1 week | 2 weeks | 6 weeks |
|---|---|---|---|
| Activated | None | miR-223 | miR-223 |
| | let-7 | let-7 | miR-122 |
| | miR-122 | miR-122 | miR-181 |
| | miR-17 | miR-135 | miR-196 |
| Inhibited | miR-148 | miR-148 | miR-21 |
| | miR-196 | miR-196 | miR-30 |
| | | miR-21 | miR-7 |
| | | miR-7 | |

miRNA/miR, microRNA; let-7, lethal-7.

Table IV. Number of genes expected to be regulated by miR-223 and miR-21 in non-alcoholic steatohepatitis liver.

| microRNA (prediction) | 1 week | 2 weeks | 6 weeks |
|---|---|---|---|
| miR-223 (activated) | None | 54 | 57 |
| miR-21 (inhibited) | None | 71 | 73 |

miR, microRNA.

*Integrated pathway analysis*. From Table III, we focused on miR-223, which was predicted to be active in expression, and miR-21, which was predicted to be repressed. The gene numbers for which these microRNAs were predicted to be involved in the regulation of gene expression were evaluated (Table IV). Based on an integrated pathway between upstream molecules and gene expression and function prediction in IPA (Fig. 3), miR-223 upregulation was predicted to enhance hepatocyte adipogenesis, cell death, inflammation, and hepatocellular injury. In contrast, miR-21 downregulation was predicted to enhance fibrosis.

*Altered expression of miR-21 and fibrosis-related gene Col3a1*. Real-time PCR was performed for miR-21, which was predicted to be associated with liver fibrosis. Significant downregulation of miR-21 expression was observed in NASH liver tissues at 1 and 2 weeks (Fig. 4A). For *Col3a1*, a gene predicted to be regulated by miR-21 and whose expression was predicted to increase over time, real-time PCR using the primers in Table V showed a significant increase in expression in NASH liver tissue at weeks 1 and 2 (Fig. 4B). This finding suggests that the expression of miR-21 in liver tissue decreased and the expression of its target, *Col3a1*, increased.

Interestingly, serum miR-21 expression and serum exosomal miR-21 were significantly increased at 1 and 2 weeks of high fat diet feeding compared to controls (Fig. 4C and D). These results suggest that miR-21 may leak from the liver into the blood during the early phase of NASH, and that fibrosis may be enhanced thereafter.

## Discussion

In the study, liver fibrosis was predicted by mRNA microarray analysis using mice fed a high-fat diet (CDAHFD) to induce NASH. Hematoxylin and eosin staining after 2 weeks showed features of NASH (inflammatory cell infiltration, fatty degeneration, and hepatocellular damage). Sirius red staining after 6 weeks showed fibrosis, and α-SMA immunohistochemical staining showed activation of hepatic stellate cells. In addition to inflammation, fibrosis was observed in mice fed CDAHFD at 6 weeks in a previous study (14). These results suggest that 2 weeks of feeding is suitable for the NASH model before fibrosis occurs and 6 weeks or later for advanced fibrosis development when the high-fat diet is used in this model.

We performed liver mRNA microarray analysis at 1, 2, and 6 weeks after high-fat diet intake and analyzed the function of genes with significant differences in IPA. When we compared histological findings with the predicted time of increased function, there was a general agreement, but the gene expression changes in liver fibrosis preceded the histological changes. The number of genes associated with liver fibrosis markedly increased from the first to 2 weeks of feeding, suggesting that gene expression changes prior to the time when fibrosis can be confirmed by pathological examination and that examining changes in fibrosis genes in liver biopsy specimens will enable prediction of future fibrosis.

The upstream regulatory molecules were selected as a relevant upstream regulatory molecule from the gene expression results. Among the upstream regulatory molecules, we focused on microRNAs, which can be analyzed using minimally invasive blood samples since the goal is to use microRNAs as fibrosis biomarkers in the future. We selected miR-223 and miR-21 as NASH-associated microRNAs. Previously, it has been reported that miR-223 is involved in cholesterol metabolism and cell apoptosis in the liver (15,16) and expression of miR-223 is altered in various liver diseases, and miR-223 expression is upregulated in liver tissue of NASH model mice (17).

Among the genes regulated by miR-21 that were predicted to be associated with liver fibrosis, we examined the expression of *Col3a1*, which was predicted to be upregulated. We found a significant increase in expression in liver tissue. *Col3a1* is a gene for type III collagen, a major component of tissues with elongation function, and accumulation of type III collagen is observed in diseases associated with fibrosis (18). In this study, *Col3a1* expression was significantly increased in the NASH group after 1 week of feeding, suggesting that fibrosis gene expression increases before 2 weeks when the onset of NASH can be confirmed by histological findings.

Decreased expression of liver miR-21 was observed very early in the development of NASH. However, it has been previously reported that increased expression of miR-21 promotes fibroblast proliferation and is associated with the development of fibrosis due to abnormal deposition of extracellular matrix (19). It is also known that miR-21 is generally overexpressed in NASH, as inhibition of liver miR-21 reduces hepatocyte damage, inflammation, and fibrogenesis (20). These reports are inconsistent with our results in the present study, suggesting that miR-21 expression in the liver may differ depending on the timing of NASH onset and the model used. On the other hand, the increase in serum miR-21 with

Table V. Primer pairs for reverse transcription-quantitative PCR.

| Primer | Sequence (5'-3') | Amplicon size, bp |
|---|---|---|
| *Gapdh* forward | GGGTTCCTATAAATACGGACTGC | 112 |
| *Gapdh* reverse | CCATTTTGTCTACGGGACGA | |
| *Col3a1* forward | GCCCACAGCCTTCTACAC | 109 |
| *Col3a1* reverse | CCAGGGTCACCATTTCTC | |

*Col3a1*, collagen type III α1.

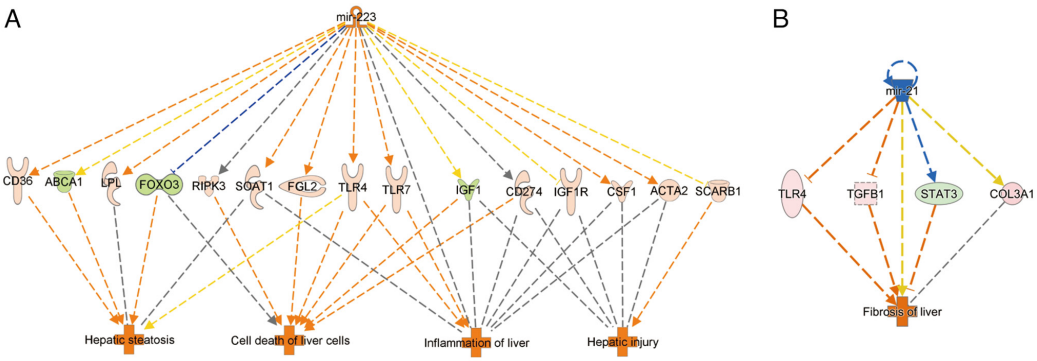


Figure 3. Integrated pathway analysis of upstream molecules, gene expression and function predictions. (A) miR-223, (B) miR-21. The top row shows each miRNA, the middle row shows the gene predicted to be regulated by each miRNA and the bottom row shows the function predicted to be involved. Orange miRNAs are upregulated, blue miRNAs are downregulated, peach genes are upregulated, green genes are downregulated and orange predicted functions are upregulated. miR, microRNA.

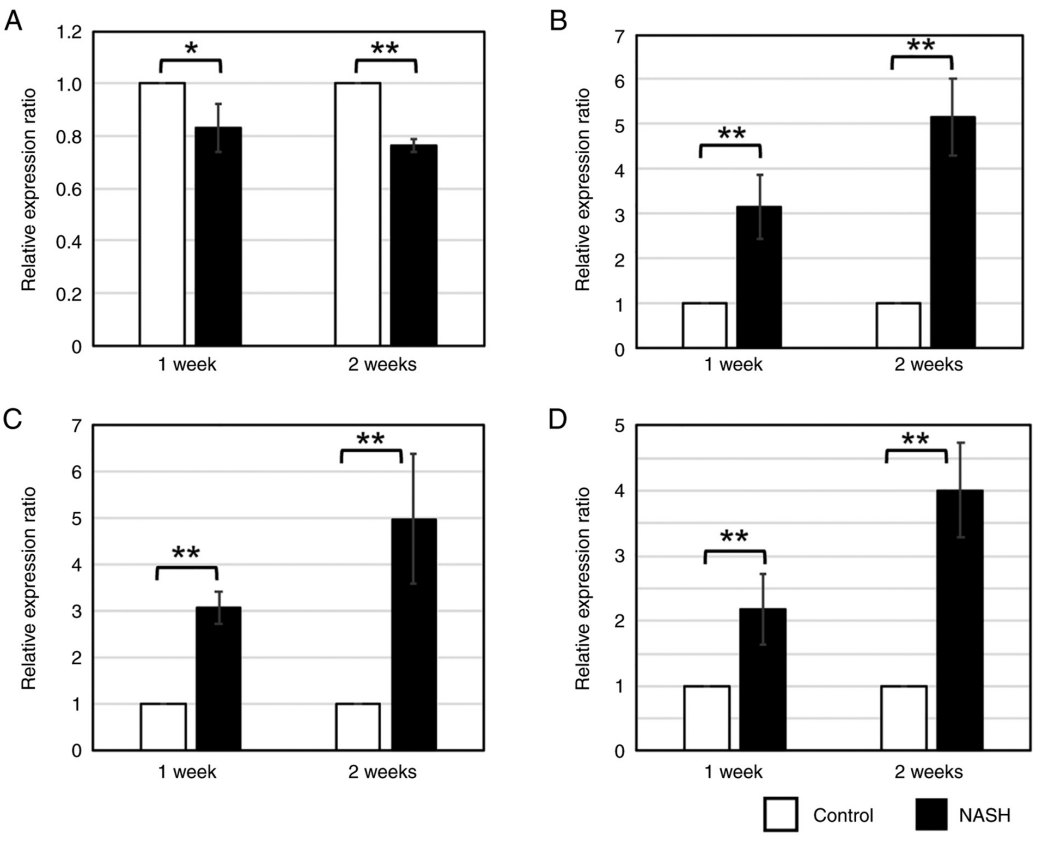


Figure 4. Gene expression of miR-21 and *Col3a1* in NASH livers and serum. Expression changes of (A) miR-21 and (B) *Col3a1* in liver tissues, and (C) miR-21 and (D) exosomal miR-21 in serum of control and NASH groups at 1 and 2 weeks. U6 snRNA and *Gapdh* were used as an internal control. Cel-miR-39 was used as an external control. Four control animals and four animals in the NASH group were evaluated. White bar presents control group, and black bar presents NASH group. $^{*}$P<0.05 and $^{**}$P<0.01. miR, microRNA; NASH, non-alcoholic steatohepatitis; *Col3a1*, collagen type III α1.

the onset of NASH was consistent with reports by other investigators (21). Therefore, monitoring blood miR-21 or exosomal miR-21 expression may be more important for fibrosis detection than miR-21 expression in the liver.

In this study, we newly showed that exosomal miR-21 in serum is increased in the blood of early NASH mice after 1 week of high-fat diet intake, suggesting the emergence of fibrosis. In the future, we would like to investigate the usefulness of serum exosomal miR-21 as a fibrosis marker.

**Acknowledgements**

Not applicable.

**Funding**

The present study was supported in part by The JSPS KAKENHI (grant nos. 21H04844 and 20K21692).

**Availability of data and materials**

The datasets used and/or analyzed during the current study are available from the corresponding author on reasonable request.

**Authors' contributions**

KM and MC were major contributors in performing the experiments and writing the manuscript. YK, MH, RM and SM helped conduct the experiments. All authors read and approved the final manuscript. KM and MC confirmed the authenticity of all the raw data.

**Ethics approval and consent to participate**

All experiments were performed in accordance with The Guidelines for Animal Experimentation of the Hirosaki University. The procedures were approved and monitored by The Animal Research Committee of Hirosaki University (approval no. G18002).

**Patient consent for publication**

Not applicable.

**Competing interests**

The authors declare that they have no competing interests.

**References**

1. Ratziu V, Bellentani S, Cortez-Pinto H, Day C and Marchesini G: A position statement on NAFLD/NASH based on the EASL 2009 special conference. J Hepatol 53: 372-384, 2010.
2. Cotter TG and Rinella M: Nonalcoholic fatty liver disease 2020: The state of the disease. Gastroenterology 158: 1851-1864, 2020.
3. Balakrishnan M and Loomba R: The role of noninvasive tests for differentiating NASH from NAFL and diagnosing advanced fibrosis among patients with NAFLD. J Clin Gastroenterol 54: 107-113, 2020.
4. Ludwig J, Viggiano TR, McGill DB and Oh BJ: Nonalcoholic steatohepatitis: Mayo clinic experiences with a hitherto unnamed disease. Mayo Clin Proc 55: 434-438, 1980.
5. Matteoni CA, Younossi ZM, Gramlich T, Boparai N, Liu YC and McCullough AJ: Nonalcoholic fatty liver disease: A spectrum of clinical and pathological severity. Gastroenterology 116: 1413-1419, 1999.
6. Brunt EM, Janney CG, Di Bisceglie AM, Neuschwander-Tetri BA and Bacon BR: Nonalcoholic steatohepatitis: A proposal for grading and staging the histological lesions. Am J Gastroenterol 94: 2467-2474, 1999.
7. Huang DQ, El-Serag HB and Loomba R: Global epidemiology of NAFLD-related HCC: Trends, predictions, risk factors and prevention. Nat Rev Gastroenterol Hepatol 18: 223-238, 2021.
8. Younossi Z, Tacke F, Arrese M, Chander Sharma B, Mostafa I, Bugianesi E, Wai-Sun Wong V, Yilmaz Y, George J, Fan J and Vos MB: Global perspectives on nonalcoholic fatty liver disease and nonalcoholic steatohepatitis. Hepatology 69: 2672-2682, 2019.
9. Argo CK, Northup PG, Al-Osaimi AM and Caldwell SH: Systematic review of risk factors for fibrosis progression in non-alcoholic steatohepatitis. J Hepatol 51: 371-379, 2009.
10. Yatsuji S, Hashimoto E, Tobari M, Taniai M, Tokushige K and Shiratori K: Clinical features and outcomes of cirrhosis due to non-alcoholic steatohepatitis compared with cirrhosis caused by chronic hepatitis C. J Gastroenterol Hepatol 24: 248-254, 2009.
11. Nagai K, Kohno K, Chiba M, Pak S, Murata S, Fukunaga K, Kobayashi A, Yasue H and Ohkohchi N: Differential expression profiles of sense and antisense transcripts between HCV-associated hepatocellular carcinoma and corresponding non-cancerous liver tissue. Int J Oncol 40: 1813-1820, 2012.
12. Tan Y, Ge G, Pan T, Wen D and Gan J: A pilot study of serum microRNAs panel as potential biomarkers for diagnosis of nonalcoholic fatty liver disease. PLoS One 9: e105192, 2014.
13. Matsumoto M, Hada N, Sakamaki Y, Uno A, Shiga T, Tanaka C, Ito T, Katsume A and Sudoh M: An improved mouse model that rapidly develops fibrosis in non-alcoholic steatohepatitis. Int J Exp Pathol 94: 93-103, 2013.
14. Toita R and Kang JH: Long-term profile of serological biomarkers, hepatic inflammation, and fibrosis in a mouse model of non-alcoholic fatty liver disease. Toxicol Lett 332: 1-6, 2020.
15. Wang L, Jia XJ, Jiang HJ, Du Y, Yang F, Si SY and Hong B: MicroRNAs 185, 96, and 223 repress selective high-density lipoprotein cholesterol uptake through posttranscriptional inhibition. Mol Cell Biol 33: 1956-1964, 2013.
16. Qadir XV, Chen W, Han C, Song K, Zhang J and Wu T: miR-223 deficiency protects against fas-induced hepatocyte apoptosis and liver injury through targeting insulin-like growth factor 1 receptor. Am J Pathol 185: 3141-3151, 2015.
17. Katsura A, Morishita A, Iwama H, Tani J, Sakamoto T, Tatsuta M, Toyota Y, Fujita K, Kato K, Maeda E, *et al*: MicroRNA profiles following metformin treatment in a mouse model of non-alcoholic steatohepatitis. Int J Mol Med 35: 877-884, 2015.
18. Kuivaniemi H and Tromp G: Type III collagen (COL3A1): Gene and protein structure, tissue distribution, and associated diseases. Gene 707: 151-171, 2019.
19. Huang Y, He Y and Li J: MicroRNA-21: A central regulator of fibrotic diseases via various targets. Curr Pharm Des 21: 2236-2242, 2015.
20. Loyer X, Paradis V, Hénique C, Vion AC, Colnot N, Guerin CL, Devue C, On S, Scetbun J, Romain M, *et al*: Liver microRNA-21 is overexpressed in non-alcoholic steatohepatitis and contributes to the disease in experimental models by inhibiting PPARα expression. Gut 65: 1882-1894, 2016.
21. Becker PP, Rau M, Schmitt J, Malsch C, Hammer C, Bantel H, Müllhaupt B and Geier A: Performance of serum microRNAs -122, -192 and -21 as biomarkers in patients with non-alcoholic steatohepatitis. PLoS One 10: e0142661, 2015.